# Polymer dynamics from large to small scales

**D. Richter**

*Institut für Festkörperforschung, Forschungszentrum Jülich, D-52425 Jülich, Germany. E-mail: neutronscattering@fz-juelich.de*

This lecture reviews quasielastic small angle neutron scattering experiments exploring the dynamics of polymer melts. Starting from the entropy driven Rouse dynamics, I address its limitation to larger and smaller scales. On the large scale side neutron spin echo spectroscopy reveals the single chain dynamic structure factor and the self correlation function of a spatially confined chain in accordance with the reptation concept and shows that contour length fluctuations limit the chain confinement on the time scale of local reptation. Towards shorter distances it is shown that intrachain dissipation processes are the leading mechanism limiting Rouse motion.

**Keywords: polymer dynamics; quasielastic neutron scattering; neutron spin echo spectroscopy**

#### 1. Introduction

The structural and dynamical properties of polymer chains are characterized by a number of different scales. The largest relates to the overall chain dimension measured by the end to end distance $R_e$ and the dynamic counter part, the overall chain diffusion. Towards smaller scales, we find a scaling or fractal regime, where independent of the chemical chain structure the polymer segments are distributed in space following laws from statistical physics (Doi & Edwards, 1986). On the dynamic side this regime is dominated by entropy driven motion – the so called Rouse dynamics – and topological confinements leading to the reptation process. In going to even smaller scales at a certain point, the detailed chemical structure of the chain becomes important and we expect a transition from global to chain specific dynamical properties. This finally leads to the relaxation processes known as $\alpha$- and $\beta$-relaxations related to the glass transition. All the dynamical processes from the overall chain diffusion to local relaxations determine the mechanical and rheological properties of polymeric materials. For any molecular design of properties it is essential to understand these phenomena on a molecular basis.

Neutrons are a nearly ideal probe for such studies since they access simultaneously the important mesoscopic length and time scales (Squires, 1978). Another key element underpinning the importance of neutrons in polymer science is the possibility of varying the contrast by hydrogen deuterium exchange. In this way both, the single chain structure factor which is observed in labeling a fraction of chains as well as the pair correlation function which is observed on a fully deuterated material, may be accessed. Finally, on protonated materials the single particle motion, the self correlation function, may be studied revealing the mean square displacement $\langle r^2(t)\rangle$ as a function of time.

Starting from the entropy driven Rouse dynamics, this lecture will explore its limits both towards large and small scales. On the large scale side neutron spin echo spectroscopy reveals the dynamic structure factor of a spatially confined polymer chain in agreement with the reptation model of De Gennes (Richter *et al.*, 1990; Butera *et al.*, 1991; Schleger *et al.*, 1998). Measurements of the mean square displacement directly reveal the cross over from the unrestricted Rouse dynamics $\langle r^2(t)\rangle \approx t^{1/2}$ to the local reptation regime $\langle r^2(t)\rangle \approx t^{1/4}$ (Monkenbusch *et al.*, 2002). NSE experiments on polymer melts of different chain lengths finally identify contour length fluctuation of the confining tube as the limiting mechanism (Wischnewski *et al.*, 2002) of local reptation. On the small scale side, the influence of local chain structure causes deviations from the Rouse dynamics. A comparative study on polydimethylsiloxane (PDMS) and polyisobutylene (PIB) two polymers exhibiting very similar static rigidities but very different orientational barriers identified dissipation processes caused by reorientational jumps as the leading mechanism (Richter *et al.*, 1999; Arbe *et al.*, 2001).

This lecture naturally is not able to review exhaustively the contribution of high resolution neutron scattering to the field of polymer melt dynamics, but rather wants in an exemplary way to display important contributions by example.

#### 2. Quasielastic neutron scattering

The most powerful technique suitable for the study of slow dynamics, the neutron spin echo spectroscopy (NSE) operates in the time domain and uncovers a time range from about 2ps to 200ns and accesses values of $Q$ (where $Q$ is the modulus of the scattering vector $\mathbf{Q} = \mathbf{k} - \mathbf{k}_0$, where $\mathbf{k}$ is the wavevector of the scattered and $\mathbf{k}_0$ the wavevector of the incident wave) between 0.01 Å$^{-1}$ and 3 Å$^{-1}$. The second important high resolution technique is neutron backscattering providing an energy resolution of up to 1μeV and covering a $Q$-range $0.1 \leq Q \leq 5$ Å$^{-1}$.

Coherent quasi- and inelastic neutron scattering reveals the dynamic structure factor $S(Q,t)$ or its Fourier transformed counterpart $S(Q,\omega)$ (Squires, 1978)

$$S(Q,t) = \frac{1}{N}\sum_{ij}\left\langle \exp\left(-i\mathbf{Q}.\mathbf{r}_j(t)\right)\exp\left(i\mathbf{Q}.\mathbf{r}_i(0)\right)\right\rangle \qquad (1)$$

where $\mathbf{r}_j(t)$ and $\mathbf{r}_i(0)$ are the position vectors of the scatterers at time $t$ and time $t = 0$ respectively, $N$ is the number of scatterers and $\hbar\mathbf{Q}$ is the momentum transfer during scattering. The brackets denote the thermal average. If a material is fully deuterated the sum in equation (1) runs over all atoms in the material. Then $S(Q,t)$ reflects the pair correlation function and relates to the collective properties of a material. In the neutron cross section it is weighted by the average scattering length $\left|\bar{b}\right|^2$. If a single chain is labeled, the double sum is restricted to the atoms of this chain and consequently $S(Q,t)$ reveals the single chain dynamic structure factor.

Incoherent scattering is related to scattering length disorder which may either origin from spin dependent scattering lengths like in the case of hydrogen or from isotope mixtures with different scattering properties. This disorder prevents constructive interference of partial waves scattered at different atoms and reveals the self correlation function. Equation (1) provides the self correlation function, if in the double sum only terms with $i = j$ are considered. In the cross section $S_{\rm inc}(Q,t)$ is weighted by the average scattering length fluctuations $\left(\left\langle b^2\right\rangle - \left|\bar{b}^2\right|\right)$.

In Gaussian approximation which is widely used for the calculation of neutron scattering functions in polymer dynamics equation (1) is approximated by

$$S(Q,t) = \frac{1}{N}\sum_{ij}\exp\left[-\frac{Q^2}{6}\left\langle\left(r_i(t)-r_j(0)\right)^2\right\rangle\right] \qquad (2)$$

  

### 3. Entropy driven dynamics - The Rouse regime

In the space time regime, where only the chain connectivity matters, the Rouse model which considers Gaussian chains in a heat bath, is the standard model of polymer dynamics (Doi & Edwards, 1986). In this model, a chain segment is subject to entropic and random forces, inertial contributions are neglected and only monomeric friction is considered. For the self motion which is observed by incoherent scattering the Rouse model predicts a mean square segment displacement

$$\left\langle r^2(t)\right\rangle = 2\ell^2\left(\frac{W}{\pi}t\right)^{1/2} \tag{3}$$

where $W$ is an elementary Rouse rate and $\ell$ a segmental length. In Gaussian approximation the incoherent scattering function monitors directly this mean-square displacement

$$S_{inc}(Q,t) = \exp\left[-\frac{Q^2}{6}\left\langle r^2(t)\right\rangle\right] \tag{4}$$

Experimentally, this behavior may be studied uniquely by neutron spin echo spectroscopy. Fig. 1 displays such results for a polyethylenepropylene (PEP) melt of a molecular weight $M_w = 80000$ at $T = 492$ K (Monkenbusch *et al.*, to be published). PEP was obtained from the hydrogenation of anionically synthesized polyisoprene. As may be seen $\left\langle r^2(t)\right\rangle$ follows beautifully the predicted time dependence. Moreover as a consequence of the spatial resolution provided, the absolute value of $\left\langle r^2(t)\right\rangle$ may directly be read off. At 22 ns, the longest time covered, $\sqrt{\left\langle r^2(t)\right\rangle}$ amounts to about 27 Å.

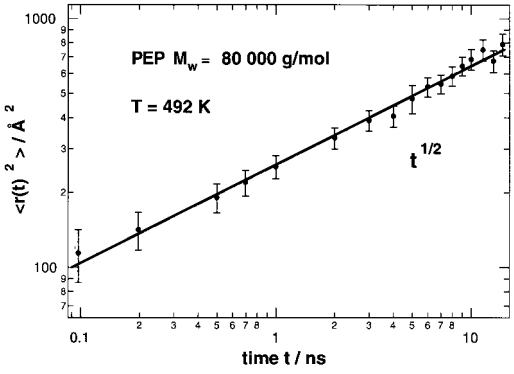


**Figure 1**
Time-dependent mean-square displacement of a PEP segment as derived from the incoherent cross section of PEP a melt via equations (3) and (4). The solid line indicates the prediction of the Rouse model.

Since in its range of applicability the Rouse dynamics is length scale free, the single chain dynamic structure factor which is obtained from a labelled chain within a matrix should follow a universal scaling law (De Gennes, 1967)

$$S(Q,t) = f\left(Q^2\ell^2\sqrt{Wt}\right) \tag{5}$$

Fig. 2 displays experiments on polyethylethylene (PEE) (Montes *et al.*, 1999) (PEE is obtained by hydrogenation from anionically synthesized 1-2 polybutadiene), where this prediction was tested. Experiments at different momentum transfers were superimposed according to equation (5). Not only the prediction is extremely well fulfilled, but also the shape of the theoretical dynamic structure factor is in very good agreement with the data.

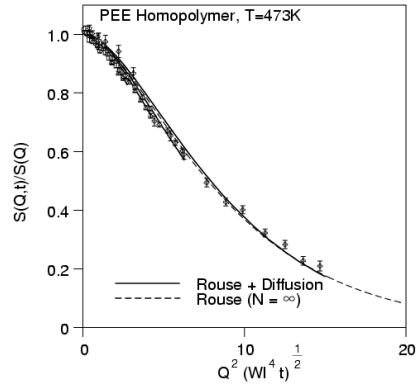


**Figure 2**
Dynamic structure factor of PEE ($M_w = 20000$) at $T = 473$ K. The data taken at different $Q$-values have been scaled following to equation (5). The various solid lines are the prediction of the Rouse model including the translational diffusion $D_t$ which appears as a multiplicative term $\exp[-DQ^2t]$ in the cross section.

### 4. Chain confinement - reptation

Entanglement formation in dense polymer systems is at the origin of their viscoelasticity and determines many mechanical properties. The most famous theory describing the topological interactions is the reptation model (De Gennes, 1971). It describes the topological hindrance to the motion of a given chain in surrounding it by a localization tube which follows the coarse grained chain profile and impedes extended lateral motion. The tube diameter $d$ in this model is identified with the entanglement distance taken from the rubber analogy of the plateau modulus. For distances smaller than $d$, the chain moves freely and exhibits Rouse dynamics, while for larger distances the chain motion is confined to the tube and the Rouse motion can only take place along the curvilinear tube. For long times the chain creeps out of the tube following its own profile; it reptates like a snake. In terms of this model, a theory of viscoelasticity has been developed which describes the main features of polymer melt rheology (Doi & Edwards, 1986).

#### 4.1 Theoretical considerations

We now consider the predictions of the reptation model for the mean square displacement of the chain segments.

(i) For short times, when the chain segment has not yet realized the topological constraints ($r < d$), we expect unrestricted Rouse motion $\left\langle \Delta r^2(t)\right\rangle \approx t^{1/2}$ (equation [3]).

(ii) For times larger than the Rouse relaxation time of an entanglement strand $\tau_e$ (i.e. a chain section of length $N_e$ the end to end distance of which equals the tube diameter $d^2 = \ell^2 N_e$; $\tau_e = \dfrac{d^4}{\ell^4\pi^2 W}$) one dimensional curve linear Rouse motion along the tube has to be considered. For times shorter

then the Rouse time $\tau_R$ of the chain ($\tau_R$ is the longest Rouse relaxation time of the whole chain) we deal with Rouse motion along the Gaussian random walk of the tube. In this local reptation regime $\langle r^2(t)\rangle = d\ell\left(\frac{W}{3}t\right)^{1/4}$ holds. For $t > \tau_R$ curve linear Rouse diffusion prevails and we get $\langle r^2(t)\rangle = d\left(\frac{W\ell}{3R_e^2}t\right)^{1/2}$, where $R_e^2$ is the end to end distance of the chain.

(iii) Finally for times larger then the reptation time $\tau_d$ at which the chain has left its original tube we expect overall chain diffusion with a mean square displacement proportional to time $\langle r^2(t)\rangle = \frac{W\ell^4 d^2}{3R_e^4}t$ .

The tube constraints also retard the relaxation of the single chain structure factor causing a near plateau regime in the time dependent single chain correlation function. Neglecting the initial free Rouse process, De Gennes has formulated a tractable expression for the dynamic structure factor which is valid for $t > \tau_e$, i.e. once confinement effects become important (Doi and Edwards, 1986; De Gennes, 1981). In the large $Q$ limit the dynamic structure factor assumes the form

$$\frac{S(Q,t)}{S(Q)} = \left(1-F(Q)\right)\exp\left(t/\tau_0\right)\operatorname{erfc}\sqrt{t/\tau_0} + F(Q)\sum_{p=1}^{N}\frac{\sin^2\alpha_p A}{\alpha_p^2\left(\mu^2+\alpha_p^2+\mu\right)}\exp\left(-\frac{4\alpha_p^2 t}{\pi^2\tau_d}\right)$$

with $F(Q) = \exp\left(-\frac{d^2Q^2}{36}\right)$ the tube "Debye Waller factor". (6)

$$\tau_0 = \frac{36}{W\ell^4Q^4} \qquad \text{the Rouse time scale}$$

$$\tau_d = \frac{3N^3}{\pi^2}\frac{\ell^2}{Wd^2} \qquad \text{the terminal time}$$

$$\alpha_p \tan\alpha_p = \mu = \frac{Q^2N\ell^2}{12}$$

and erfc $x$ = 1 - erf $x$ and $A$ is a normalisation factor.

For short times $S(Q,t)$ decays mainly due to local reptation (first term), while for longer times (and low $Q$) the second term resulting from the creep motion dominates. The ratio of the two relevant time scales $\tau_0$ and $\tau_d$ is proportional to $N^3$. Therefore, for long chains at intermediate times $\tau_e < t < \tau_d$ a pronounced plateau in $S(Q,t)$ is predicted.

Such a plateau is a signature for confined motion and is present also in other models for confined chain motion. Besides the reptation model also other entanglement models have been brought forward. We discuss them briefly by categories.

1. In generalized Rouse models, the effect of topological hindrance is described by a memory function. In the border line case of long chains the dynamic structure factor can be explicitly calculated in the time domain of the NSE experiment. In this class fall entanglement models by Ronca (Ronca, 1983), Hess (Hess, 1986; 1987; 1988) Chaterjee and Loring (Chatterjee & Loring, 1994).

2. Rubber like models take entanglements literally as temporary cross links. Such an approach has been brought forward by Des Cloizeaux (Des Cloizeaux, 1993). He assumes that the entanglement points between chains are fixed as in a rubber and that under the boundary condition of fixed entanglements the chains perform Rouse motion. This rubber like model is conceptually closest to the idea of a temporary network.

3. In a mode coupling approach a microscopic theory describing the polymer motion in entangled melts has been developed. While these theories describe well the different time regimes for segmental motion, unfortunately as a consequence of the necessary approximations a dynamic structure factor could not yet been derived (Schweizer, 1989).

#### 4.2 Experimental observations of chain confinement – Single chain structure factor

Fig. 3 compares the dynamic structure factors from polyethylene melts, both taken at 509 K for two different molecular weights (Richter *et al.*, 1993; Wischnewski *et al.*, 2002). Fig. 3(*a*) displays the structure factor for a short chain melt ($M_w$ = 2000 g/mol). The solid lines display a fit with the Rouse dynamic structure factor. Again very good agreement is achieved. Fig. 3(*b*) displays similar results from a PE melt with a molecular weight of $M_w$ = 12400 g/mol. The solid lines present the predictions of the Rouse model. While for the short chain melts, this model describes sufficiently well the experimental observations for the longer chains the model fails completely. Only in the short time regime the initial decay of the dynamic structure factor is depicted while for longer times the relaxation behaviour is strongly retarded signifying confinement effects.

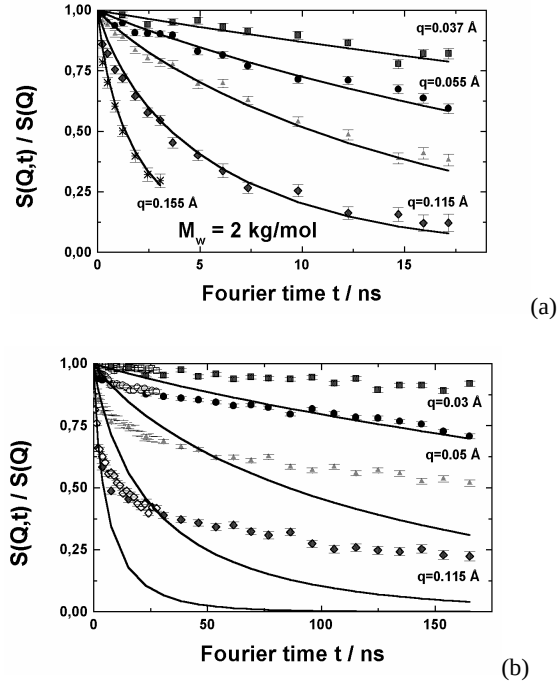


**Figure 3**
Dynamic structure factors from PE-melts at 509 K (a) $M_w$ = 2000; (b) $M_w$ = 12400. The solid lines display the predictions of the Rouse model.

Fig. 4 presents recent experimental results on a polyethylene melt ($M_w$ = 190000) which were carried over a time regime of 170ns (Schleger *et al.*, 1998). The data are compared with the dynamic structure factor of the reptation model (equation (6)) which fits very well. We note, that the fits were performed varying only a single parameter, namely the tube diameter $d$ while the Rouse rate was determined from earlier NSE data taken at short times. With this one parameter it is possible to achieve quantitative agreement both with respect to the $Q$ and the time dependence of the dynamic structure factor. We further note, that the dynamic structure factors predicted by the other confinement models discussed above are not able to fit the data.

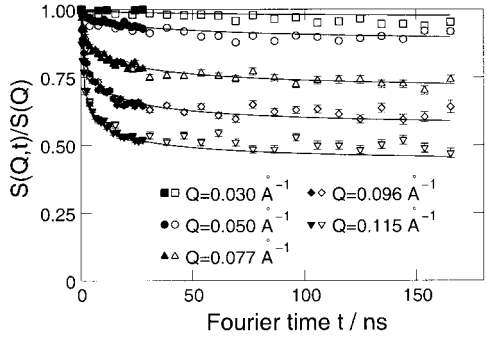


**Figure 4**
Dynamic structure factor from a long chain PE-melt ($M_w$ = 190000) at 509 K. The solid lines represent a fit with the reptation model (equation (6)).

It is illustrative to visualize the large spread of the time regimes relevant for the dynamics of the $M_w$ = 190000 molecule. The elementary Rouse time amounts to 2.5 ps. The cross over time to local reptation $\tau_e$ = 6 ns. The Rouse time of the chain $\tau_R$ = 45 μs and finally the disentanglement time $\tau_d$ = 11.7 ms. Thus, the relevant times scales spread over a range of more than nine orders of magnitude. The corresponding length scales are much closer together. The segment length $\ell = \ell_0\sqrt{C_\infty}$, where $C_\infty$ is the characteristic ratio, is 4 Å, the tube diameter $d$ = 48 Å and the chain end-to-end distance $R_e$ = 418 Å (Schleger *et al.*, 1998).

#### 4.3 Experimental observation of chain confinement- mean square displacements

We now turn to the mean square displacement of a chain segment, which may be observed by incoherent quasielastic scattering (Monkenbusch *et al.*, to be published). Here, in the local reptation regime we expect a cross over of the time dependent mean square displacement from a $t^{1/2}$- to a $t^{1/4}$-law.

Experimentally such incoherent neutron spin echo experiments are extremely difficult. The reasons are that

(i) incoherent scattering is emitted into the full solid angle 4π,
(ii) with the incoherent scattering in two thirds of the scattering events a spin flip of the neutron spin occurs reducing the echo signal from +1 to $-^1/_3$.

This reduced signal sits on a high background caused by the spin flipped neutrons. In order to perform such experiments, very long counting times and an extremely stable instrument are necessary.

Fig. 5 presents the time dependent mean square displacement obtained from the same $M_w$ = 190000 PE sample as studied also in the coherent measurement. $\langle r^2(t)\rangle$ was evaluated using the Gaussian approximation equation (2). Experiments have been performed at two different $Q$ values and the corresponding mean square displacements are plotted double logarithmically against the time. The two solid lines display the expected asymptotic $t^{1/2}$- and $t^{1/4}$-time laws. As may be seen, the data display a pronounced cross over from a $t^{1/2}$ behavior at short times to a $t^{1/4}$ law at longer times. At first sight surprisingly, a cross over was found at a time $\tau_e$ = 0.8 ns corresponding to a tube diameter $d$ = 30 Å in strong disagreement with the value of 48 Å from the dynamic structure factor experiment.

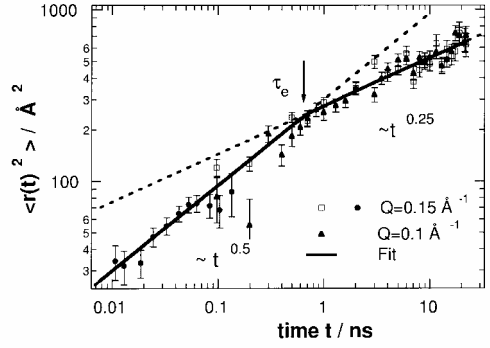


**Figure 5**
Time dependent mean square displacement from a $M_w$ = 190000 PE-melt at 509 K assuming the Gaussian approximation $\langle r^2(t)\rangle = -\frac{6}{Q^2}\ln S(Q,t)$. The solid dashed lines display the $t^{1/2}$- and $t^{1/4}$-laws respectively.

The origin of this discrepancy is of rather subtle nature (Fatkullin & Kimmich, 1995) and relates to the Gaussian approximation which was taken in order to extract $\langle \Delta r^2(t)\rangle$ from equation (2). For a curve linear motion along a contorted tube this Gaussian assumption is not valid. While the curve linear displacement inside the tube have a Gaussian character, the real space displacements strongly deviate from this behaviour. If this effect is taken into account the discrepancies are removed and both the self as well as the pair correlation function lead to the same tube diameter and cross over times (Monkenbusch *et al.*, to be published).

#### 4.4 Contour length fluctuations

Now, we ask for the effect of the chain length on chain confinement (Wischnewski *et al.*, 2002). For this purpose, NSE experiments were performed on polyethylene melts spanning a molecular weight range from 12.4 kg/mol up to 190 kg/mol. Fig. 6 displays the result. We first qualitatively discuss the data and compare the spectra at $Q$ = 0.115 Å$^{-1}$. For the highest molecular weights at $M_w$ = 190 kg/mol and $M_w$ = 36 kg/mol the spectra are characterized by an initial fast decay reflecting the unconstraint dynamics at early times and very pronounced plateaus for $S(Q,t)$ at later times signifying the tube constraints. The plateau values for the two samples are practically identical. Inspecting the results for smaller $M_w$ we realize that

(i) the dynamic structure factors decays to lower values (0.5 at $M_w$ = 190 kg/mol, 0.4 at $M_w$ = 24.7 kg/mol and nearly 0.2 at $M_w$ = 12.4 kg/mol);
(ii) furthermore, the long time plateaus start to slope the more the smaller $M_w$ becomes, with $M_w$ = 12.4 kg/mol nearly loosing the

plateau in $S(Q,t)$. Obviously, the chains are disentangling from the tube and the constraints are successively removed.

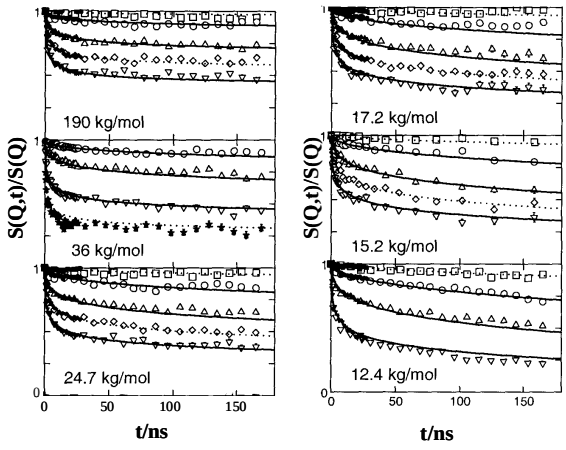


**Figure 6**
Neutron spin echo spectra from the polyethylene melts of various molecular weights. The $Q$ values correspond to squares, $Q = 0.003$ Å$^{-1}$; circles, $Q = 0.005$ Å$^{-1}$, triangles (up), $Q = 0.077$ Å$^{-1}$; diamonds, $Q = 0.096$ Å$^{-1}$; triangles (down), $Q = 0.115$ Å$^{-1}$; crosses, $Q = 0.15$ Å$^{-1}$. Filled symbols refer to a wavelength of the incoming neutrons $\lambda = 8$ Å and open symbols refer to $\lambda = 15$ Å. For lines, see explanation in text.

If the data are analysed using the pure reptation model of equation (6) a tube diameter $d$, which increases with decreasing molecular weight is obtained. This is displayed in Fig. 7, where the tube diameter is plotted as a function of molecular weight. We observe an increase from about 45 to 60 Å. Secondly, it is found (not shown here) that the quality of the fit is decreasing with decreasing molecular weight.

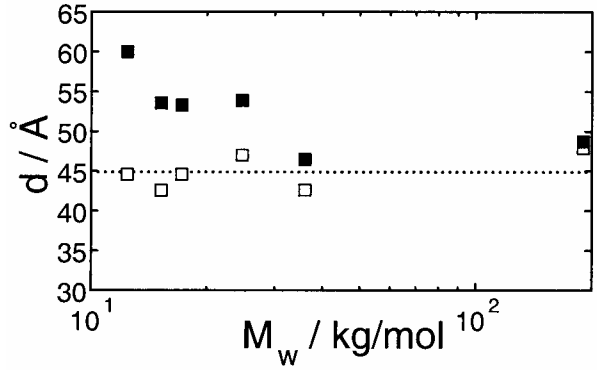


**Figure 7**
Resulting tube diameters from the model fits with pure reptation (filled squares) and reptation and contour-length fluctuations (open squares) as a function of molecular weight. The dotted line is a guide for the eye.

As it is known from the broad a cross over phenomena observed in the macroscopic chain dynamics such as the molecular weight dependence of the melt viscosity very important limiting mechanism exist which effect the confinement limit of the reptation process. These processes increase in importance as the chain length decreases. In the time regime $t < \tau_R$, theoretically, tube contour length fluctuations removing the tube constraints from the ends have been identified as the most important limiting process. For times $t < \tau_R$ the fraction of monomers released from the tube due to contour length fluctuations has a simple form

$$\Psi(t) = \frac{1.5}{Z}\left(\frac{t}{\tau_e}\right)^{1/4} \tag{7}$$

where $Z = N/N_e$ is the number of entanglements per chain.

Following the approach of Clarke and McLeish (Clarke & McLeish, 1993), this result may be incorporated into the structure factor of equation (6). It replaces the second part and yields.

$$S(Q,t) = F(Q)\frac{1}{2\mu^2}\left[2\mu + e^{-2\mu} + 2 - 4\mu s(t) - 4e^{-2\mu s(t)} + e^{-4\mu s(t)}\right] \tag{8}$$

where $\mu$ has been defined in equation (6) and $s(t) = \psi(t)/2$.

The lines in Fig. 6 display the result of a fit with equation (8). A group of three common $Q$ values for all molecular weights is displayed by thick solid lines to facilitate the easy comparison of the molecular weight dependence of the curves. Additional $Q$ values only available for some values of $M_w$ are represented by dotted lines.

The open squares in Fig. 7 show the resulting tube diameters. Aside from small fluctuations they now stay constant independent of $M_w$. While at the highest molecular weight contour lengths fluctuations are insignificant and both lines of fitting yield the same $d$, at the smallest $M_w = 12.4$ kg/mol, the difference in the fitted tube diameters between both approaches rises to nearly 30% emphasizing the strong effect of contour length fluctuations in loosening the grip of the entanglements on a given chain. Thus, the comparison between the experimental chain length dependent dynamic structure factor and theoretical predictions clearly show, that for times $t < \tau_R$ contour length fluctuations are the leading mechanism that limits the chain confinement inherent to the reptation picture. Without any further assumptions or fitting parameters – the tube diameter d stays constant with $M_w$ - it is possible to describe the full $M_w$ dependence of $S(Q,t)$ in terms of local reptation and the contour length fluctuation mechanism. Even for chain lengths corresponding to only 6-7 entanglements the tube diameter appears to be a well defined quantity assuming the same value as for asymptotically long chains. The confinement is lifted from the chain ends inwards, while the chain center remains confined in the original tube.

#### 5. Intermediate scale dynamics

A precondition for the validity of the entropy driven Rouse model is the requirement that only chain connectivity enters into the equation of motion and any influence from local stiffness or rotational barriers etc. is negligable. In going to shorter length scales this condition must break down. Measurements of the dynamic structure factor at smaller scales or higher $Q$-values offer the opportunity to learn about the limitation of the Rouse model towards local scales and to understand the leading processes. Both local chain stiffness as well as rotational potentials may play a role (Allegra & Ganazzoli, 1981; 1989, Harnau *et al*., 1995; 1996).

Recently, the relevant factors which limit the universal Rouse dynamics towards small scales were studied in comparing the dynamic structure factors $S(Q,t)$ of polyisobutylene (PIB) and polydimethylsiloxane (PDMS) molecules of similar size in the melt

and in dilute solution (Richter *et al.*, 1999; Arbe *et al.*, 2001). Both polymers show similar static flexibility (the characteristic ratios are very close), but strongly different rotational barriers (PDMS: $E_{rot} \cong 0.1$ kcal/mol; PIB: $E_{rot} = 3$ kcal/mol).

Fig. 8(*a*) presents the dynamic structure factor from a PIB melt at 470 K including a fit with the prediction of the Rouse model. Fig. 8(*b*) displays comparable data from a PDMS melt at 373 K.

While for *Q*-values above $Q = 0.15$ Å$^{-1}$ increasing deviations between the experimental results from PIB and the Rouse prediction are evident, the PDMS results are described well over the entire *Q*-range (up to $Q = 0.4$ Å$^{-1}$). Since both polymers exhibit the same static flexibility, we may immediately conclude, that chain stiffness is not the leading mechanism limiting the Rouse dynamics for flexible polymers as proposed earlier (Harnau *et al.*, 1995; 1996). A thorough study of the stiffness effects on the dynamics of this polymer was carried out in (Richter *et al.*, 1999) applying the approaches of the all rotational state model and a bending force model. Stiffness effects were found to be almost neglible.

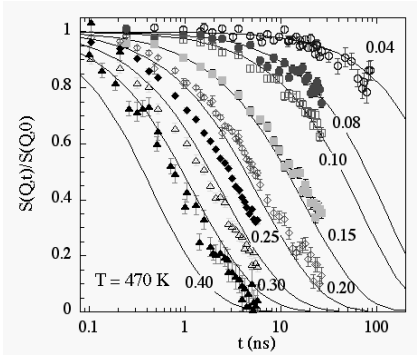


**Figure 8**
Dynamic structure factor of (*a*) a PIB melt ($M_w = 3870$, $M_w/M_n = 1.06$, radius of gyration $R_g = 19.2$ Å) at 470 K and (*b*) of a PDMS melt ($M_w = 6460$, $M_w/M_n = 1.10$, $R_g = 21.3$ Å) at 373 K (○: $Q = 0.04$ Å$^{-1}$; ●: $Q = 0.08$ Å$^{-1}$; □: $Q = 0.10$ Å$^{-1}$; ■: $Q = 0.15$ Å$^{-1}$; ◇: $Q = 0.20$ Å$^{-1}$; ◆: $Q = 0.25$ Å$^{-1}$; △: $Q = 0.3$ Å$^{-1}$; ▲: $Q = 0.4$ Å$^{-1}$). The solid lines the respective predictions of the Rouse model.

After the failure of stiffness models, the source for the slowing down of the PIB chain dynamics at intermediate scales must be related to dissipation effect not present in PDMS. Allegra's intrachain viscosity model (Allegra & Ganazzoli, 1981; 1989) provides a simplified access to such an effect. He describes the intrachain dissipation degrees of freedom - mainly rotational transitions across barriers - by a local relaxation mode characterized by a relaxation time $\tau_0$.

In order to access this process without disturbances, experiments on solutions were crucial, where interchain friction effects are weak (Arbe *et al.*, 2001). Fig. 9 compares experimental results on PIB and PDMS in toluene at room temperature and at 370 K. While at low *Q* both data sets agree – both polymers undergo the same translational diffusion – at larger *Q* a systematic retardation of the dynamic response of PIB compared to PDMS is visible.

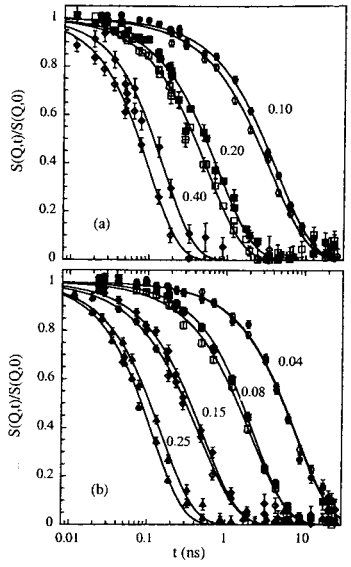


**Figure 9**
Chain dynamic structure factor of PDMS (empty symbols) and PIB (full symbols - in each case the lower curve) in toluene solution at 300 K (*a*) and 370 K (*b*). The corresponding *Q* values are indicated. Lines through the points are guides to eye.

The application of the intrachain viscosity model to the PIB solution data on the basis of the PDMS reference led to a very good description of the NSE results for all *Q* values and temperatures (Fig. 10). The activation energy of 3.1 kcal/mol for the intrachain relaxation time $\tau_0$ agrees very well with the rotational barrier for this hydrocarbon (Dejean *et al.*, 1989, Jones *et al.*, 1978; Inoue *et al.*, 1973).

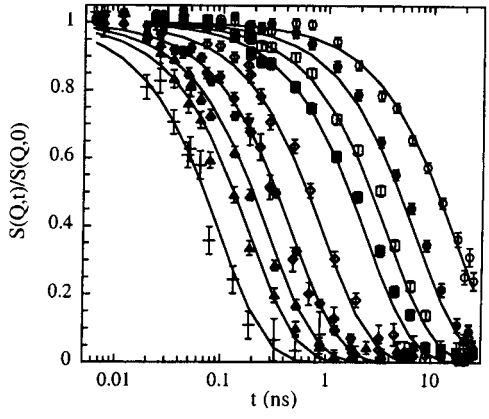


**Figure 10**
Chain dynamic structure factor PIB in toluene solution at 327 K at the *Q* values: 0.04 Å$^{-1}$ (○); 0.06 Å$^{-1}$ (●); 0.08 Å$^{-1}$ (□); 0.10 Å$^{-1}$ (■); 0.15 Å$^{-1}$ (◇); 0.20 Å$^{-1}$ (◆); 0.25 Å$^{-1}$ (△); 0.30 Å$^{-1}$ (▲); 0.40 Å$^{-1}$ (+). Solid lines correspond to fitting curves with the Rouse-Zimm model including intrachain viscosity.

An application of the model to the melt data allows a quantitative description of the $Q$-dependent spectra. The activation energy for $\tau_0$ resulted to be about 10 kcal/mol, more than 3 times as high as in solution. Obviously chain relaxation occurs via correlated motions over several barriers or interchain effects come in additionally and the activation energy cannot easily be compared with rotational potentials.

Thus, Allegra's intrachain viscosity model accounts properly for the deviations from universal dynamics. In solution the corresponding relaxation time directly relates to jumps across rotational potentials. Also in the melt intrachain friction effects limit the Rouse dynamics. The relaxation time, however, is not directly related to crossings of single barriers.

#### 6. Summary and conclusions

In this lecture, we have discussed the dynamics of polymer melts restricting ourself to homopolymers. We have covered the range of molecular motions starting in the sub Rouse regime to large scale motions reaching the size of the entire chain. The lecture attempted to transmit a flavor of what can be achieved with high resolution neutron spectroscopy, which permits the access to molecular motion simultaneously in space and time.

The lecture commenced with a description of the standard model of polymer motion, the entropy driven dynamics, covered by the Rouse model. In the spatial range, where the detailed chemical structure of the monomers ceases to be of importance NSE measurements have well confirmed the predictions of the Rouse model both for the self and the pair correlation functions.

Towards larger scales topological interactions resulting from the mutually interpenetrating chains gain dominant influence and confine the chain motion to a tube along the chain profile. We have presented measurements of the dynamic structure factor of a reptating chain which unequivocally confirm the picture of local reptation i.e. Rouse relaxation along a contorted tube. A measurement of the self correlation function corroborates this picture – both experiments may be interpreted by the same set of parameters. With decreasing chain length, the tube confinement looses its grip and tube length fluctuations free the motions of the chain ends. This picture inherent in the reptation approach was also corroborated by NSE studies.

Towards shorter length scales in the regime, where the picture of universal chain dynamics governed by entropic forces ceases to be valid, the limiting mechanisms were identified by NSE studies. It turned out that intrachain dissipation mechanisms related to rotational jumps between different isomeric states limit the Rouse process towards shorter distances.

Though, this lecture restricted itself to homopolymer melts, I hope to have shown that the investigation of polymer dynamics is a broad and rich field with a great potential. Neutrons play a key role in such investigations, because they allow to perform observations on the proper length and time scales as well as to exercise hydrogen deuterium contrast variation. Further developments will go in the direction of time dependent phenomena and real time experiments.

We will look on nonequilibrium and transient phenomena, on the complexity posed by multicomponent systems, on molecular rheology, in order to understand the functioning of materials, and we will try to find a bridge to biology.

I am very thankful to a large number of scientist who made this interdisciplinary work possible. In particular I like to mention the colleagues from chemistry L.J. Fetters (Cornell), L. Willner and J. Allgaier (Jülich), from experimental physics M. Monkenbusch and A. Wischnewski (Jülich), A. Arbe and J. Colmenero (San Sebastian) and B. Farago (Grenoble). Theoretical advice from T.C.B. McLeish and A. Likhtman (Leeds) is gratefully acknowledged.

#### References

Allegra, G. & Ganazzoli, F. (1981). *Macromolecules* **14**, 1110-1119.

Allegra, G. & Ganazzoli, F. (1989). *Advances in Chemical Physics* **75**, 265-348.

Arbe, A., Monkenbusch, M., Stellbrink, J., Richter, D., Farago, B., Almdal, K. & Faust, R. (2001). *Macromolecules* **34**, 1281-1290.

Butera, R., Fetters, L.J., Huang, J.S., Richter, D., Pyckhout-Hintzen, W., Zirkel, A., Farago, B., Ewen, B. (1991). *Phys. Rev. Lett.* **66**, 2088-2091.

Chatterjee, A., Loring, R. (1994). *J. Chem. Phys.* **101**, 1595-1606.

Clarke, N. & McLeish, T.C.B (1993). *Macromolecules* **26**, 5264-5266.

De Gennes, P.G. (1967). *Physics (USA)* **3**, 37-45.

De Gennes, P.G. (1971). *J. Chem. Phys.* **55**, 572-579.

De Gennes, P.G. (1981). *J. Phys. Paris* **42**, 735-740.

Dejean de la Batie, R., Lauprêtre, F. &. Monnerie, L. (1989). *Macromolecules* **22**, 2617-2622.

Des Cloizeaux, J. (1993). *J. Phys. I Fr.* **3**, 1523-1539.

Doi, M. & Edwards, S.F. (1986). *The theory of polymer dynamics*, Clarendon, Oxford, UK.

Fatkullin, N. & Kimmich, R. (1995). *Phys. Rev.* E**52**, 3273-3276.

Harnau, L., Winkler, R.G. & Reinicker, P.J. (1995). *J. Chem. Phys.* **102**, 7750-7757.

Harnau, L., Winkler, R.G. & Reinicker, P.J. (1996). *J. Chem. Phys.* **104**, 6355-6368.

Hess, W. (1986). *Macromolecules* **19**, 1395-1404.

Hess, W. (1987). *Macromolecules* **20**, 2587-2599.

Hess, W. (1988). *Macromolecules* **21**, 2620-2632.

Inoue, Y., Nishioka, A. & Chûjô R. (1973), *J. Polym. Sci.; Polym. Phys. Ed.* **11**, 2237-2252.

Jones, A.A., Lubianez, R.P., Hanson, M.A. &. Shostak, S.L.J. (1978). *J. Polym. Sci.; Plym. Phys. Ed.* **16**, 1685-1701.

Monkenbusch, M., Wischnewski, A., Willner, L. & Richter, D. (2002). To be published.

Montes, H., Monkenbusch, M., Willner L., Richter D., Fetters, L.J., Rathgeber, S. & Farago, B. (1999). *J. Chem. Phys.* **110**, 10188-10202.

Richter D., Farago B., Fetters, L.J., Huang, J.S., Ewen, B., Lartigue, C. (1990). *Phys. Rev. Lett.* **64**, 1389-1392.

Richter, D., Monkenbusch, M., Allgaier, J., Arbe, A., Colmenero, J., Farago, B., Cheol, Y. & Faust, R. (1999). *J. Chem. Phys.* **111**, 6107-6120.

Richter, D., Willner L., Zirkel, A., Farago, B., Fetters, L.J. & Huang, J.S. (1993). *Phys. Rev. Lett.* **71**, 4158-4161.

Ronca, G. (1983). *J. Chem. Phys.* **79**, 1031-1043.

Schleger, P., Farago, B., Kollmar, A., Lartigue, C. & Richter D. (1998). *Phys. Rev. Lett.* **81**, 124-127.

Schweizer, K.S. (1989). *J. Chem. Phys.* **91**, 5802-5821.

Schweizer, K.S. (1989). *J. Chem. Phys.* **91**, 5822-5839.

Squires, G.L. (1978). *Introduction to the theory of thermal neutron scattering*, Cambridge University Press, Cambridge, UK.

Wischnewski, A., Monkenbusch, M., Willner, L., Richter, D., Likhtman, A.E., McLeish, T.C.B. & Farago B. (2002). *Phys. Rev. Lett.* **88**, 058301-1 – 058301-4.

 Received 29 August 2002 • Accepted 3 March 2003 